

Proceedings of the
**SIXTH (1987) INTERNATIONAL
OFFSHORE MECHANICS AND ARCTIC
ENGINEERING SYMPOSIUM**

presented at

THE SIXTH (1987) INTERNATIONAL
SYMPOSIUM & EXHIBIT ON OFFSHORE
MECHANICS AND ARCTIC ENGINEERING
HOUSTON, TEXAS
MARCH 1-6, 1987

organized by

OMAE Symposium Technical Program
Committee and ASME - Offshore
Mechanics and Arctic Engineering Division

sponsored by

American Society of Mechanical Engineers, USA
Society of Naval Architects of Japan, Japan
Institution of Mechanical Engineers, United Kingdom
London Centre for Marine Technology, United Kingdom
Norwegian Society of Chartered Engineers, Norway
Chinese Society of Ocean Engineers, China
Chinese Society of Naval Architects and
Marine Engineers, China
Conseil de Liaison des Associations de
Recherche sur les Ouvrages en Mer, France
The Japan Society of Mechanical Engineers, Japan
Japanese Society of Civil Engineers, Japan
Dansk Ingenioerforening, Denmark
Korea Committee for Ocean Resources
and Engineering, Korea
Italian Association for Marine and Offshore
Engineers, Italy
Deutsches Komitee fur Meeresforschung und
Meerestechnik, e.V., Federal Republic of Germany
Canadian Society for Mechanical Engineers, Canada
Society of Steel Construction for Japan, Japan
Architectural Institute of Japan, Japan
The Iron and Steel Institute of Japan, Japan
The Marine Engineering Society in Japan, Japan
The Japan Petroleum Institute, Japan
The Japanese Association for Petroleum
Technology, Japan
National Science Foundation, USA

VOLUME I

OFFSHORE TECHNOLOGY

Compliant Structures
Deepwater Production Systems and Structures
Riser Mechanics and Design
Mooring Systems and Anchors
Offshore Drilling and Structures
ROV and Structural Damage

GEOTECHNICAL ENGINEERING

Pile Foundations and Pile-Structure Interactions
Gravity Structure Foundation

Marine Soil and Soil Behaviors

OCEAN ENERGY TECHNOLOGY

edited by

JIN S. CHUNG

Colorado School of Mines
Golden, Colorado

CH. P. SPARKS

Institut Francais du Petrole
Rueil Malmaison, France

T. NOGAMI

University of California
La Jolla, California

T. R. CHARI

Memorial University of Newfoundland
St. John's, Newfoundland, Canada

T. R. PENNEY

Solar Energy Research Institute
Golden, Colorado

THE AMERICAN SOCIETY OF MECHANICAL ENGINEERS
United Engineering Center 345 East 47th Street New York, N.Y. 10017

DYNAMIC SOIL-STRUCTURE INTERACTION ANALYSIS OF OFFSHORE GRAVITY PLATFORMS USING SIMPLIFIED MODEL

T. Nogami
University of California
San Diego, California

M. B. Leung
Exxon Production Research Company
Houston, Texas

ABSTRACT

In the analytical formulation of dynamic response of offshore gravity platforms, a new mechanical model is proposed to represent the foundation medium underneath the basemat of the platform. The approach utilizes vertically oriented beam members interconnected by a system of springs to model the soil. The parameters of the model can be determined logically from the material properties of the foundation medium for complex foundation profiles. Using the proposed foundation model, the dynamic response of a massless rigid basemat is formulated in simple closed form. Good agreement is found in the comparison of results computed by the proposed approach with those computed by other approaches. The dynamic response of offshore gravity platforms is studied using the proposed approach for foundation modeling. The study demonstrates that the response of the platform is sensitive to the foundation behavior, especially to the soil profile and the location of the bedrock. The study concludes that an accurate representation of the foundation is very important in determining the dynamic response of gravity platforms, and that the proposed approach is an efficient tool to fulfill this need.

INTRODUCTION

Offshore structures are subjected to various dynamic loads during their design life. Dynamic loads are most typically induced by waves and sometimes by earthquakes or other sources. The response of a structure to dynamic loads depends to some extent on the behavior of the foundation due to the soil-structure interaction effect. Stiff structures, such as offshore gravity structures, are particularly sensitive to this interaction effect. Therefore, the soil-structure interaction effect must be accurately accounted for in the dynamic analysis of gravity platforms.

The behavior of the foundation is often characterized by the foundation stiffness and damping. Various methods have been developed for the evaluation of these quantities. Mathematically, the most rigorous way to evaluate these properties is to use the wave equation solutions (1, 2, 6, 8, 9). Unfortunately,

numerical evaluation of the wave equation solution involves complex mathematics, and is therefore limited to problems with simple soil profiles. On the other hand, the evaluation of the foundation properties may be accomplished by using a finite element method to accommodate complex soil profiles (2, 7, 14). The computational effort required is fairly insensitive to the complexity of the soil profile. However, regardless of the simplicity of the soil profile, the finite element method requires a large computational effort and therefore has limited applications such as two-dimensional analysis.

Another approach to evaluate the foundation stiffness and damping is to simplify the foundation medium by using simple mechanical models. A Winkler model is the simplest of all but fails to reproduce the foundation behavior as a continuous medium. To overcome this deficiency, two-parameter models have been proposed (4, 13). A major uncertainty with this approach, however, is to relate the parameters in the mechanical model with the actual material properties of the foundation medium, in particular for a complex profile subjected to dynamic loading. Recently, a new model has been developed by extending a conventional two-parameter model (10, 12). The parameters of this model can be determined logically from material properties of the foundation medium regardless of the complexity of the soil profile. Also, these parameters can be selected logically to reflect the dynamic loading condition (11). This paper presents this new method and its application on the dynamic soil-structure interaction analysis of offshore gravity platforms.

DYNAMIC RESPONSE OF OFFSHORE GRAVITY PLATFORMS

Figure 1 shows an offshore gravity platform subjected to dynamic loads such as wave loads and seismic ground excitations. The equation of motion of this structure can be written as

$$\begin{aligned}
 [M] (\ddot{U}) + [C] (\dot{U}) + [K] (U) - \ddot{X} [M] (1) + (P) \\
 M_o \ddot{U}_o + (1)^T [M] (U) - Q_u - \ddot{X} (1)^T [M] (1) - \ddot{X} M_o \\
 + (1)^T (P) (1)
 \end{aligned} \quad (1)$$

$$I_0 \ddot{\psi}_0 + (h)^T [M] (\dot{U}) - Q_\psi - \ddot{X} (h)^T [M] (1) + (h)^T (P)$$

where [M], [C] and [K] are the mass, damping and stiffness matrices for a fixed base platform, respectively; M_0 and I_0 are the mass and mass moment of inertia of the basemat; (\ddot{U}) , (\dot{U}) and (U) are vectors containing the accelerations, velocities and displacements of the platform excluding those of the basemat, respectively; U_0 and ψ_0 are horizontal and rotational accelerations of the basemat, respectively; (h) is the vector containing the heights of the masses excluding the basemat mass; \ddot{X} is the free-field ground surface acceleration due to earthquake; Q_u and Q_ψ are soil reaction forces resulting from the lateral and rotational motions of the basemat, respectively.

It is shown in the next section that, by using the proposed simplified soil model, the reaction forces Q_u and Q_ψ can be expressed as linear functions of U_0 and ψ_0 , respectively. By substituting the expressions of Q_u and Q_ψ into Eq. 1, the response of the platform can then be determined.

SOIL REACTION FORCES

Governing Equation

This section presents the governing equation that determines the soil reactions for a horizontally layered soil medium underlain by a rigid bedrock. Each of the layers is modeled by vertical beams interconnected by distributed horizontal springs as shown in Fig. 2. Although the model can easily be extended to a 3-D model, a plane strain 2-D model is considered herein. Under vertical loads, the beams are assumed to move only in an axial direction and the horizontal springs produce shear forces between two adjacent beams. On the other hand, under horizontal loads, the beams are assumed to move laterally due to the shear and the horizontal springs produce normal forces between two adjacent beams.

It is shown in Ref. 11 that the properties of the beam and uniformly distributed springs in a single model unit representing a unit width of the layer are related to the soil properties through

$$\begin{aligned} m &= \rho g_v(\nu) && \text{for vert. beam response} \\ &= \rho g_h(\nu) && \text{for horiz. beam response} \\ k_D &= E^* g_v(\nu) f_n(\nu) && \text{for vert. beam response} \\ &= E^* g_h(\nu) f_s(\nu) && \text{for horiz. beam response} \\ k_s &= 0.5 E^* g_v(\nu) f_s(\nu) && \text{for vert. beam response} \\ &= E^* g_h(\nu) f_n(\nu) && \text{for horiz. beam response} \end{aligned} \quad (2)$$

where m is the mass per unit length of the beam; k_D is the stiffness of the beam per unit length; k_s is the stiffness of the distributed springs per unit length of the beam; E^* , ρ and ν are complex Young's modulus, mass per unit volume, and Poisson's ratio of the soil, respectively; $g_v(\nu)$ and $g_h(\nu)$, which are given in Ref. 11, are about one for $\nu < 0.35$ and less than one for $\nu > 0.35$, and

$$\begin{aligned} f_n(\nu) &= (1 - \nu) / [(1 + \nu)(1 - 2\nu)] \\ f_s(\nu) &= 1 / [2(1 + \nu)] \end{aligned}$$

Assuming a linear variation of displacement with depth within each particular layer, the equation of motion for a particular layer of thickness l can be written as (11)

$$\begin{aligned} -[N^L] \begin{bmatrix} U_1''(x,t) \\ U_2''(x,t) \end{bmatrix} + [K^L] \begin{bmatrix} U_1(x,t) \\ U_2(x,t) \end{bmatrix} + [M^L] \begin{bmatrix} \ddot{U}_1(x,t) \\ \ddot{U}_2(x,t) \end{bmatrix} \\ - \begin{bmatrix} q_1(x,t) \\ q_2(x,t) \end{bmatrix} \end{aligned} \quad (3)$$

where $q_1(x,t)$ and $q_2(x,t)$ are forces distributed at the upper and lower ends of the layer, respectively; $U_1(x,t)$ and $U_2(x,t)$ are displacements of the layer at the upper and lower ends of the layer, respectively, and

$$\begin{aligned} U''(x,t) &= \frac{\partial^2 U(x,t)}{\partial x^2} \\ \ddot{U}(x,t) &= \frac{\partial^2 U(x,t)}{\partial t^2} \\ [N^L] &= \frac{m l}{6} \begin{bmatrix} 2 & 1 \\ 1 & 2 \end{bmatrix} \\ [K^L] &= k_D / l \begin{bmatrix} 1 & -1 \\ -1 & 1 \end{bmatrix} \\ [M^L] &= \frac{l k_s}{6} \begin{bmatrix} 2 & 1 \\ 1 & 2 \end{bmatrix} \end{aligned} \quad (4)$$

Obtaining Eq. 3 for all layers and applying the compatibility and equilibrium conditions at the interfaces between the layers, the equation of motion of the entire layered system is finally expressed as

$$-[N] \{ U''(x,t) \} + [K] \{ U(x,t) \} + [M] \{ \ddot{U}(x,t) \} = \{ q(x,t) \} \quad (5)$$

where $\{ U(x,t) \}$ is the vector containing the displacements of the layers (i.e., displacements at the upper-end of each layer); $[N]$, $[K]$ and $[M]$ are square matrices with a size equal to the number of the layers, and are obtained by superimposing $[N^L]$, $[K^L]$ and $[M^L]$ of all layers as illustrated in Fig. 3.

Solutions of The Governing Equation

The solutions of the governing equation for both horizontal and rotational excitations are derived in this section. The solution for vertical excitation can be derived in a similar approach. Figure 4 shows a rigid basemat of an offshore platform with a width $2d$ subjected to a harmonic lateral or rotational excitation. The soil medium is divided into three regions as shown in Fig. 4. The equation of motion of the soil medium in the left and right areas is given by Eq. 5 with $\{ q(x,t) \} = \{ 0 \}$. Solving Eq. 5 for a displacement amplitude $\{ U(x) \}$, and using the relationships $\{ T(x) \} = [N] \{ U'(x) \}$, in which $\{ T(x) \}$ is the vector of spring forces acting at the sides of the beam (side force), the following force-displacement relationship at the boundaries CD and EF can be derived:

$$\{ T^{L,R} \} = [S] \{ U^{L,R} \} \quad (6)$$

where $\{ U^L \}$ and $\{ U^R \}$ are vectors containing displacements at CD of the left area and at EF of the right area, respectively; $\{ T^L \}$ and $\{ T^R \}$ are vectors containing the side forces acting on CD of the left area and EF of the right area, respectively. Equation 6 can be split into

$$T_A^{L,R} = S_{AA} U_A^{L,R} + \tilde{S}_{AB}^T \tilde{U}_B^{L,R} \quad (7a)$$

$$T_B^{L,R} = \tilde{S}_{BA} U_A^{L,R} + \tilde{S}_{BB} \tilde{U}_B^{L,R} \quad (7b)$$

where T_A and U_A are the side force and displacement of the top layer, respectively, and T_B and U_B are the side forces and displacements for the rest of the layers, respectively. Hence,

$$[S] = \begin{bmatrix} S_{AA} & \tilde{S}_{AB}^T \\ \tilde{S}_{BA} & \tilde{S}_{BB} \end{bmatrix}; \quad \{ T \} = \begin{bmatrix} T_A \\ T_B \end{bmatrix}; \quad \{ U \} = \begin{bmatrix} U_A \\ U_B \end{bmatrix} \quad (8)$$

where \tilde{S}_{AB} and \tilde{S}_{BA} are vectors with a size equal to the total number of layers minus one.

The behavior of the soil at the central area is governed by Eq. 5 with

$$\{q(x,t)\} = \begin{bmatrix} q_A(x,t) \\ 0 \end{bmatrix} \quad \text{and} \quad \{U''(x,t)\} = \begin{bmatrix} 0 \\ \tilde{U}''_B(x,t) \end{bmatrix}$$

where $q_A(x,t)$ is the contact pressure between the basemat and soil, and $\tilde{0}$ is the vector containing zeros. Hence, for steady state harmonic motion, Eq. 5 for the central area can be split into

$$-\tilde{N}_{AB}^T \tilde{U}''_B(x) + R_{AA} U_A(x) + \tilde{R}_{AB}^T \tilde{U}''_B(x) = q_A(x) \quad (9a)$$

$$-\tilde{N}_{BB} \tilde{U}''_B(x) + \tilde{R}_{BB} \tilde{U}''_B(x) = -\tilde{R}_{BA} U_A(x) \quad (9b)$$

where $U_A(x) = U_0$ for horizontal response, and $U_A(x) = x \psi_0$ for rotational response, and R_{AA} , \tilde{R}_{AB}^T , \tilde{R}_{BA} and \tilde{R}_{BB} are partitions of $[R]$ such that

$$[R] = \begin{bmatrix} R_{AA} & \tilde{R}_{AB}^T \\ \tilde{R}_{BA} & \tilde{R}_{BB} \end{bmatrix} \quad (10)$$

and $[R]$ is defined as $[R] = [K] - \omega^2 [M]$, where ω is the circular excitation frequency.

A general solution for $\tilde{U}''_B(x)$ can be obtained from Eq. 9b with $U_A(x) = U_0$ for horizontal response and $U_A(x) = x \psi_0$ for rotational response. The vertical shear force $\tilde{T}_B(x)$ can be obtained by $\tilde{T}_B(x) = \tilde{N}_{BB} \tilde{U}''_B(x)$. The expressions for $\tilde{U}''_B(x)$ and $\tilde{T}_B(x)$ contain unknown constants, which are determined from the boundary conditions at CD and EF (e.g. $\tilde{U}''_B(-d) = \tilde{U}''_B^L$, $\tilde{U}''_B(d) = \tilde{U}''_B^R$, $\tilde{T}_B(-d) = \tilde{T}_B^L$ and $\tilde{T}_B(d) = \tilde{T}_B^R$). After the unknown constants are determined, $\tilde{U}''_B(x)$ can be expressed in the form of

$$\begin{aligned} \tilde{U}''_B(x) &= \tilde{\lambda}_u(x) U_0 && \text{for horizontal response} \\ &= \tilde{\lambda}_\psi(x) x \psi_0 && \text{for rotational response} \end{aligned} \quad (11)$$

where $\tilde{\lambda}_{u,\psi}(x)$ is the matrix determined by solving the unknown constants. The expression for $\tilde{\lambda}_{u,\psi}(x)$ is given in Ref. 11.

Equilibrium condition of a rigid base requires

$$\begin{aligned} Q_u &= T_A^L + T_A^R + \int_{-d}^d q_A(x) dx \\ Q_\psi &= -d T_A^L + d T_A^R + \int_{-d}^d [x q_A(x)] dx \end{aligned} \quad (12)$$

Substituting Eqs. 7a, 9a and 11 into Eq. 12, Eq. 12 can be rewritten as

$$\begin{aligned} Q_u &= 2 (S_{AA} + \tilde{S}_{AB}^T \tilde{\lambda}_u(-d) + R_{AA} d + \int_0^d (-\tilde{R}_{AB} \tilde{\lambda}_u''(x) + \tilde{R}_{AB}^T \tilde{\lambda}_u(x)) dx) U_0 \\ Q_\psi &= 2d (S_{AA} + \tilde{S}_{AB}^T \tilde{\lambda}_\psi(-d) + R_{AA} d^2/3 + (1/d) \int_0^d x^2 (-\tilde{R}_{AB} \tilde{\lambda}_\psi''(x) + \tilde{R}_{AB}^T \tilde{\lambda}_\psi(x)) dx) \psi_0 \end{aligned}$$

The integrations of $\tilde{\lambda}_{u,\psi}(x)$, $\tilde{\lambda}_{u,\psi}''(x)$, $x \tilde{\lambda}_{u,\psi}(x)$ and $x \tilde{\lambda}_{u,\psi}''(x)$ over x are given in closed form in Ref. 11.

ASSESSMENT OF PRESENT APPROACH

Foundation stiffness and damping values were calculated by the present approach and compared with those computed by other solutions using more rigorous approaches. Figure 5 shows the comparison between the prediction by the proposed method with the finite element results computed by Tassoulas (14) for a

homogenous visco-elastic medium underlain by a rigid base. In Fig. 5, β is the material damping ratio, G and ν are the shear modulus and Poisson's ratio of soil, respectively, and a_0 is defined as $d\omega/V_s$, where V_s is the shear wave velocity of soil. Good agreement can be seen generally. It is noted that the present approach did not predict the second minor peak in a horizontal response. It is because this minor peak corresponds to the resonance involving vertical soil motion and the present approach assumes no vertical motion in the soil medium when the foundation is subjected to horizontal excitation. The validity of the proposed simplified approach is also assessed in an example involving a nonhomogeneous soil profile illustrated in Fig. 6. The results computed by Gazetas using the wave propagation equation solution (5) were used for comparison. Again, good agreement between the two results validates the present approach.

APPLICATION EXAMPLES

The soil and structural data of typical deepwater gravity platforms on soft soil were used in this example, which are shown in Fig. 7. The superstructure was idealized as a vertical rigid beam system with a single mass. The weight was assumed to be 75,600 KN (17,000 K) located at 100 m (330 ft) above the foundation. The basemat was assumed to be rigid and 187 m (614 ft) wide. In computing the dynamic response of the platform in this example, the soil reaction forces to the basemat were calculated by using three different soil models: (1) Model A developed by the proposed simplified method, (2) Model B based on elastic half space solutions under plane strain conditions (3), in which the damping includes both radiation and material damping, and (3) Model C with frequency independent spring defined for static conditions and dashpot reflecting material damping only. In brief, Model B ignores the presence of the bedrock and the variation of soil properties with depth, Model C does not account for the frequency dependency of the dynamic properties of the foundation, and Model A is the most accurate modeling of the foundation among the three models.

Figure 8 compares the spring stiffness and the equivalent dashpot constants of the three different models for various frequencies. Model C gives constant lateral and rocking stiffness that match the stiffness of Model A at very low frequencies. The dashpot constants of Model C also match those of Model A closely for low frequencies, indicating that for low frequencies the damping predicted by the simplified soil model comes from the soil material damping. This is consistent with the observation that for a stratum overlaying a bedrock, radiation damping is absent for frequencies lower than the fundamental frequency of the stratum. At frequencies higher than the fundamental resonant frequency of the stratum (0.8 cps), waves propagate laterally to infinity and therefore Model A begins to vary from Model C.

By comparing the damping ratios of Models A and B, it is concluded that if a layered stratum is approximated as a homogenous half space, the radiation damping is unrealistically over-estimated by a factor of two to three times. This is consistent with the observation that the layering of soil and the presence of bedrock greatly reduce the amount of radiation damping from that calculated for the homogenous half space. The spring stiffnesses for the homogenous half space (i.e. Model B) are fairly close to the other two models for low frequencies, and only vary slightly for higher frequencies.

A unit harmonic load was applied laterally at a height of 192 m (630 ft) above the foundation. The response of the tower at this location was then calculated by solving Eq. 1. The results for the three

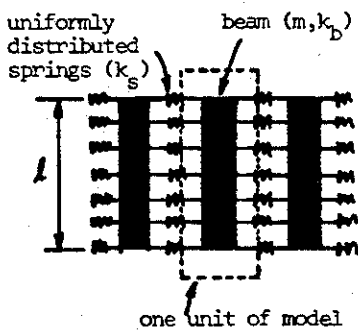
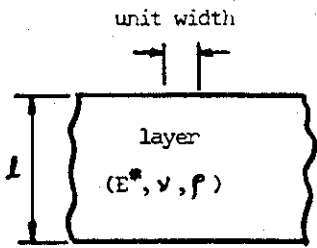


Figure 2 Simplified Model for a Layer of Soil

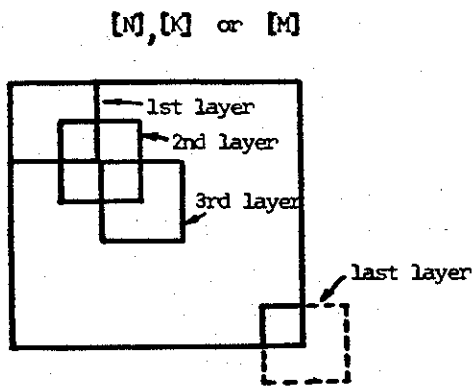


Figure 3 Construction of Global Matrices [N], [K], and [M] from Layers

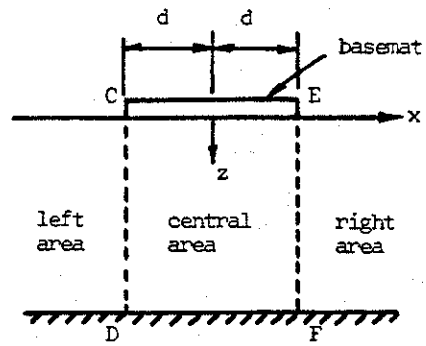


Figure 4 Divided Regions for Foundation Soil Medium

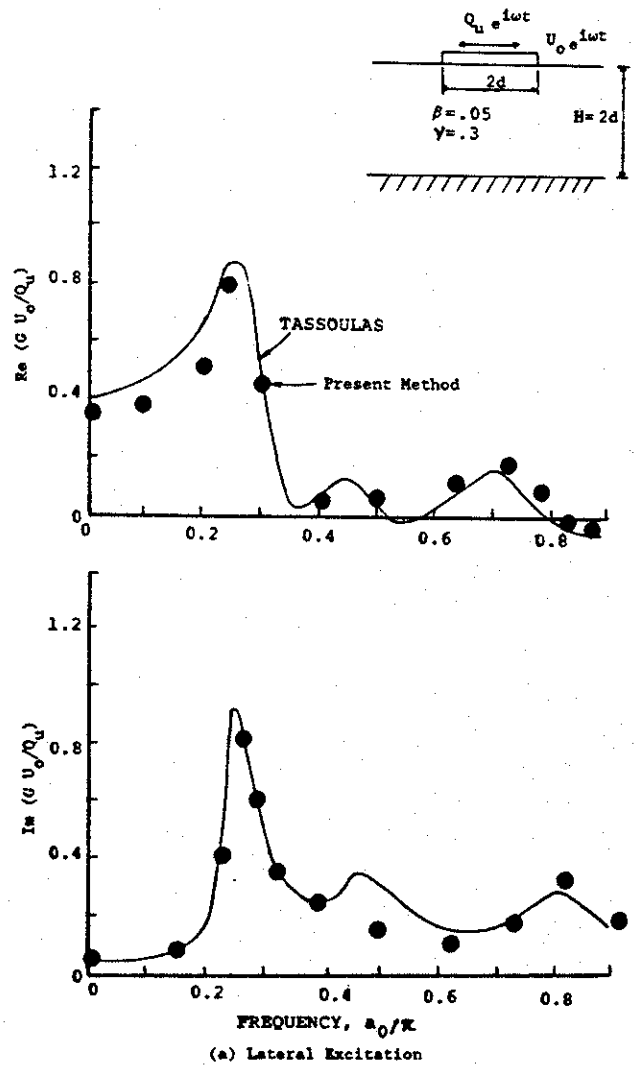
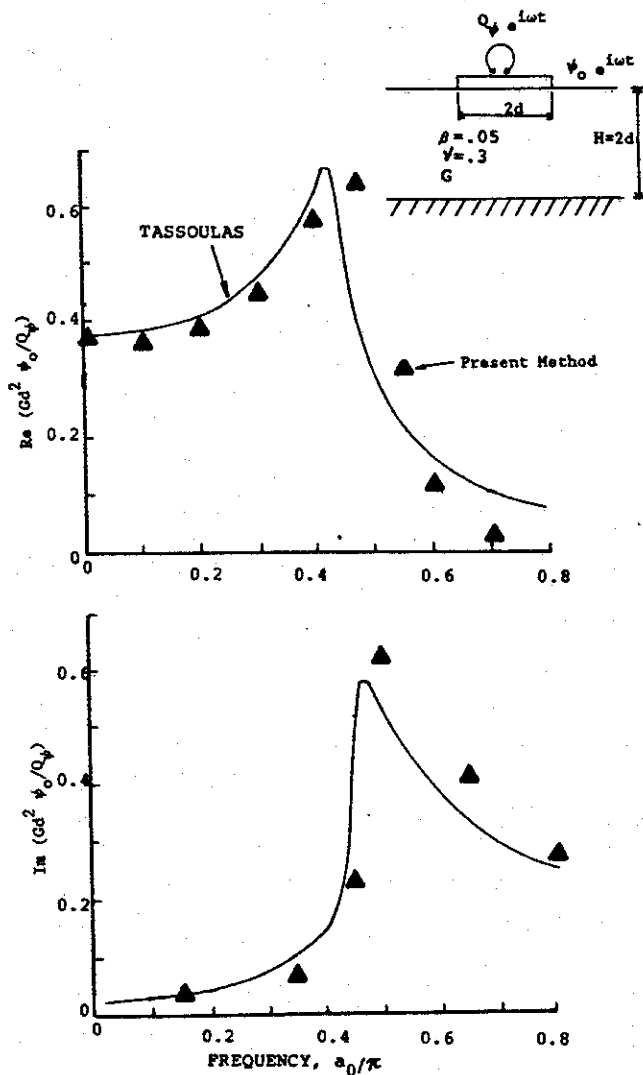


Figure 5 Verification of the Present Method for Homogeneous Soil Underlain by Bedrock



(b) Rocking Excitation

Figure 5 Verification of the Present Method for Homogeneous Soil Underlain by Bedrock

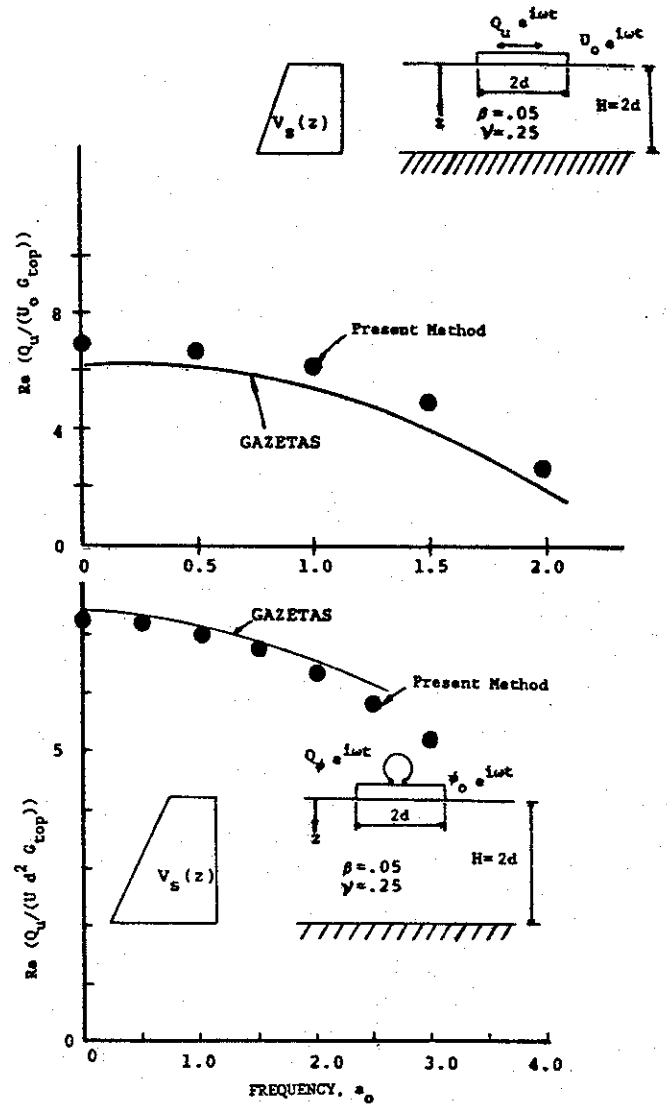


Figure 6 Verification of the Present Method for Inhomogeneous Soil Underlain by Bedrock

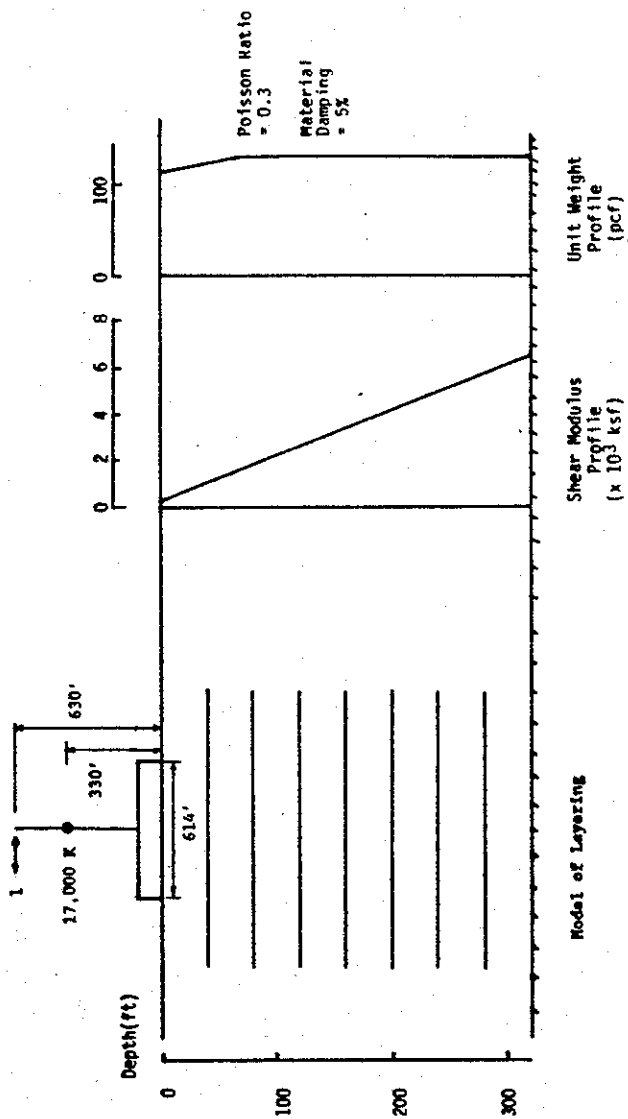


Figure 7 Foundation and Soil Properties for Example Problem

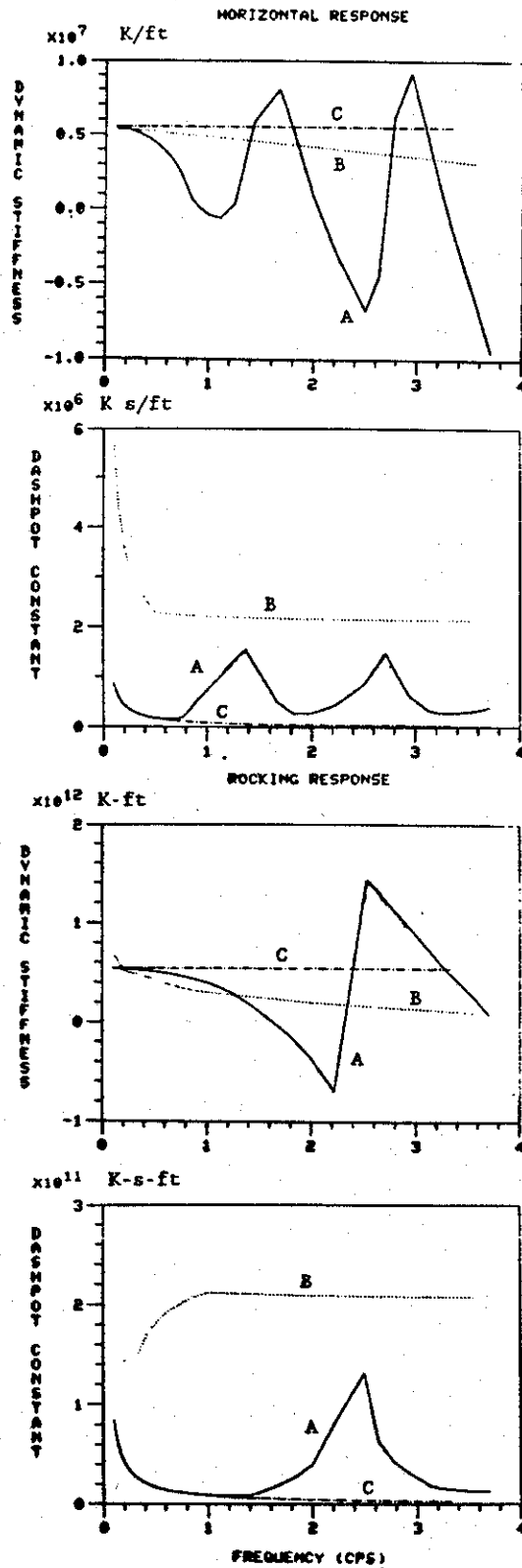


Figure 8 Spring Stiffnesses and Dashpot Constants for Foundation Models

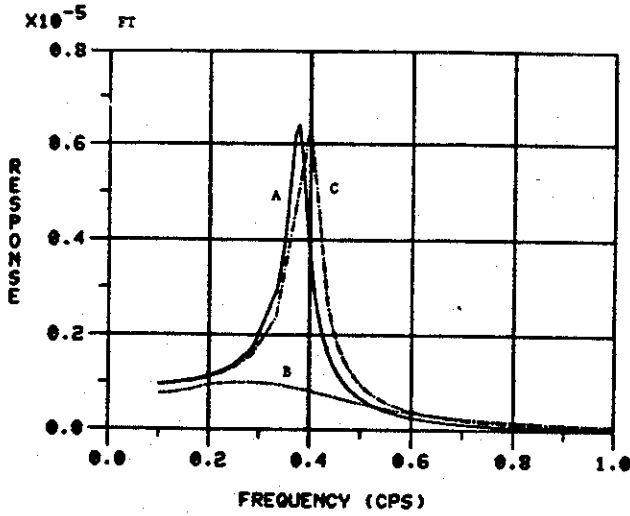


Figure 9 Response of the Tower for Different Foundations Models

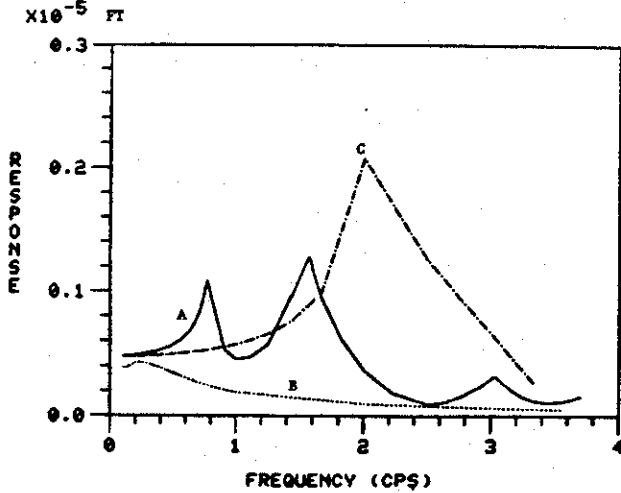


Figure 10 Response of the Tower (with Reduced Mass and Height) for Different Foundations Models

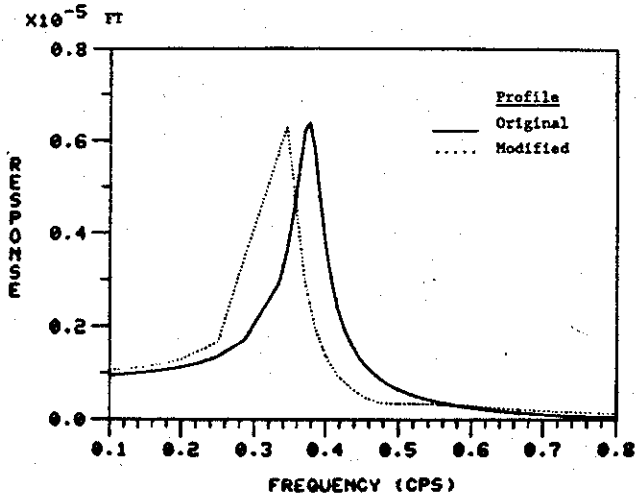


Figure 12 Response of the Tower for the Original and Modified Soil Profiles

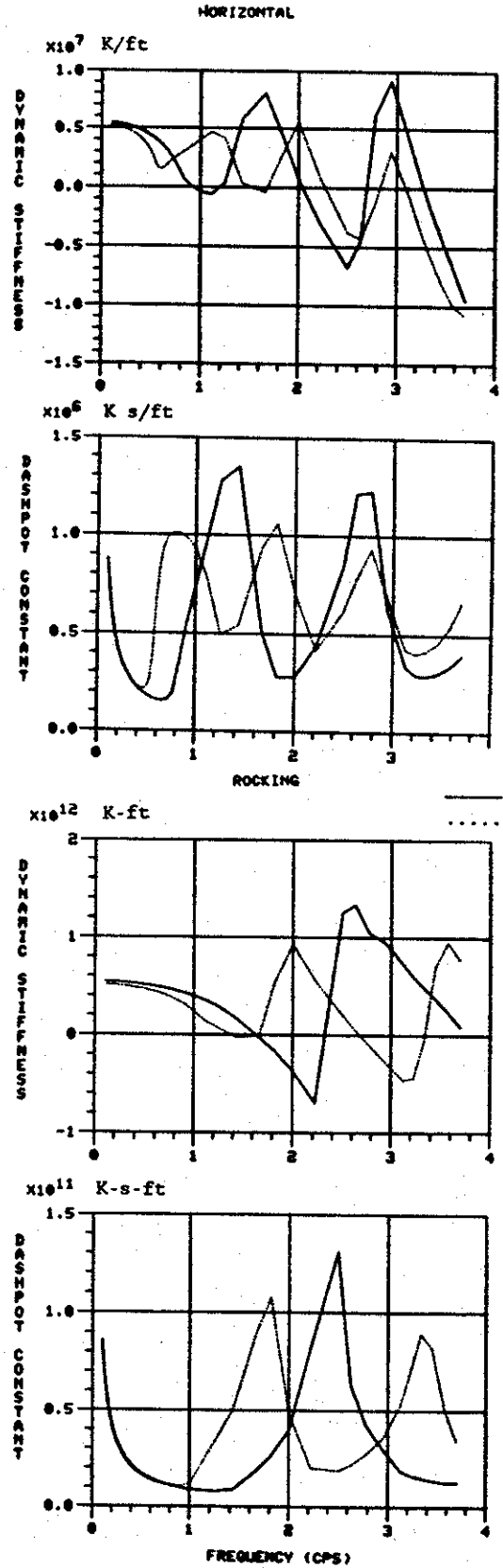


Figure 11 Spring Stiffnesses and Dashpot Constants for Original and Modified Soil Profiles